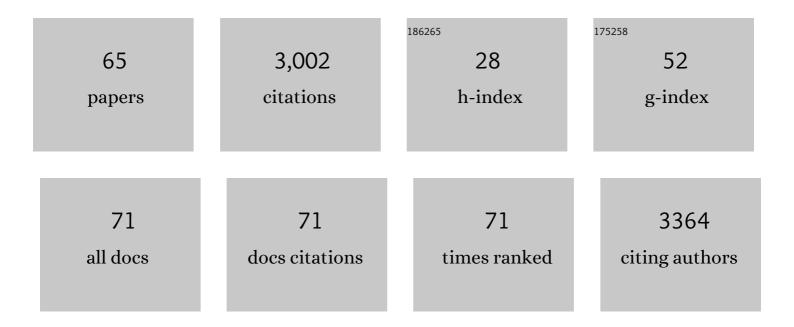
## Da-Fu Chen

List of Publications by Year in descending order

Source: https://exaly.com/author-pdf/6681634/publications.pdf Version: 2024-02-01



#	Article	IF	CITATIONS
1	Soft Conducting Polymer Hydrogels Cross-Linked and Doped by Tannic Acid for Spinal Cord Injury Repair. ACS Nano, 2018, 12, 10957-10967.	14.6	246
2	Fundamental Theory of Biodegradable Metals—Definition, Criteria, and Design. Advanced Functional Materials, 2019, 29, 1805402.	14.9	226
3	Promoting inÂvivo early angiogenesis with sub-micrometer strontium-contained bioactive microspheres through modulating macrophage phenotypes. Biomaterials, 2018, 178, 36-47.	11.4	194
4	A Tough and Self-Powered Hydrogel for Artificial Skin. Chemistry of Materials, 2019, 31, 9850-9860.	6.7	151
5	Injectable PLGA microspheres with tunable magnesium ion release for promoting bone regeneration. Acta Biomaterialia, 2019, 85, 294-309.	8.3	136
6	Near-Infrared Light Triggered Phototherapy and Immunotherapy for Elimination of Methicillin-Resistant <i>Staphylococcus aureus</i> Biofilm Infection on Bone Implant. ACS Nano, 2020, 14, 8157-8170.	14.6	133
7	Exosomes‣oaded Electroconductive Hydrogel Synergistically Promotes Tissue Repair after Spinal Cord Injury via Immunoregulation and Enhancement of Myelinated Axon Growth. Advanced Science, 2022, 9, e2105586.	11.2	117
8	Role of Cu element in biomedical metal alloy design. Rare Metals, 2019, 38, 476-494.	7.1	110
9	3D printed silk-gelatin hydrogel scaffold with different porous structure and cell seeding strategy for cartilage regeneration. Bioactive Materials, 2021, 6, 3396-3410.	15.6	110
10	Selfâ€Adaptive Antibacterial Porous Implants with Sustainable Responses for Infected Bone Defect Therapy. Advanced Functional Materials, 2019, 29, 1807915.	14.9	82
11	Lysozyme-Assisted Photothermal Eradication of Methicillin-Resistant <i>Staphylococcus aureus</i> Infection and Accelerated Tissue Repair with Natural Melanosome Nanostructures. ACS Nano, 2019, 13, 11153-11167.	14.6	74
12	A pH-sensitive self-healing coating for biodegradable magnesium implants. Acta Biomaterialia, 2019, 98, 160-173.	8.3	73
13	An injectable, self-healing, electroconductive extracellular matrix-based hydrogel for enhancing tissue repair after traumatic spinal cord injury. Bioactive Materials, 2022, 7, 98-111.	15.6	73
14	Enhanced Osseointegration of Zn-Mg Composites by Tuning the Release of Zn Ions with Sacrificial Mg-Rich Anode Design. ACS Biomaterials Science and Engineering, 2019, 5, 453-467.	5.2	70
15	3D Printing of Mechanically Stable Calciumâ€Free Alginateâ€Based Scaffolds with Tunable Surface Charge to Enable Cell Adhesion and Facile Biofunctionalization. Advanced Functional Materials, 2019, 29, 1808439.	14.9	62
16	Tunable Mechanical, Antibacterial, and Cytocompatible Hydrogels Based on a Functionalized Dual Network of Metal Coordination Bonds and Covalent Crosslinking. ACS Applied Materials & Interfaces, 2018, 10, 6190-6198.	8.0	61
17	A novel biomedical titanium alloy with high antibacterial property and low elastic modulus. Journal of Materials Science and Technology, 2021, 81, 13-25.	10.7	61
18	In vivo antibacterial property of Ti-Cu sintered alloy implant. Materials Science and Engineering C, 2019, 100, 38-47.	7.3	59

#	Article	IF	CITATIONS
19	What controls the antibacterial activity of Ti-Ag alloy, Ag ion or Ti2Ag particles?. Materials Science and Engineering C, 2020, 109, 110548.	7.3	59
20	The rapid photoresponsive bacteria-killing of Cu-doped MoS <sub>2</sub> . Biomaterials Science, 2020, 8, 4216-4224.	5.4	57
21	Formation Mechanism, Corrosion Behavior, and Cytocompatibility of Microarc Oxidation Coating on Absorbable High-Purity Zinc. ACS Biomaterials Science and Engineering, 2019, 5, 487-497.	5.2	52
22	HIF-1α Inhibits Wnt Signaling Pathway by Activating Sost Expression in Osteoblasts. PLoS ONE, 2013, 8, e65940.	2.5	49
23	Effect of ultrasonic micro-arc oxidation on the antibacterial properties and cell biocompatibility of Ti-Cu alloy for biomedical application. Materials Science and Engineering C, 2020, 115, 110921.	7.3	48
24	Synergistic Inhibition of Wnt Pathway by HIF-1α and Osteoblast-Specific Transcription Factor Osterix (Osx) in Osteoblasts. PLoS ONE, 2012, 7, e52948.	2.5	47
25	3D printing of Cu-doped bioactive glass composite scaffolds promotes bone regeneration through activating the HIF-11± and TNF-1± pathway of hUVECs. Biomaterials Science, 2021, 9, 5519-5532.	5.4	43
26	Strontium modulates osteogenic activity of bone cement composed of bioactive borosilicate glass particles by activating Wnt/l²-catenin signaling pathway. Bioactive Materials, 2020, 5, 334-347.	15.6	42
27	Osteoblast-specific transcription factor Osterix (Osx) and HIF-1α cooperatively regulate gene expression of vascular endothelial growth factor (VEGF). Biochemical and Biophysical Research Communications, 2012, 424, 176-181.	2.1	38
28	Hyaluronic acid facilitates bone repair effects of calcium phosphate cement by accelerating osteogenic expression. Bioactive Materials, 2021, 6, 3801-3811.	15.6	38
29	Mechanical Stimulation on Mesenchymal Stem Cells and Surrounding Microenvironments in Bone Regeneration: Regulations and Applications. Frontiers in Cell and Developmental Biology, 2022, 10, 808303.	3.7	30
30	Effect of cyclic mechanical loading on immunoinflammatory microenvironment in biofabricating hydroxyapatite scaffold for bone regeneration. Bioactive Materials, 2021, 6, 3097-3108.	15.6	29
31	COX2 is involved in hypoxia-induced TNF- $\hat{1}\pm$ expression in osteoblast. Scientific Reports, 2015, 5, 10020.	3.3	27
32	0D/1D Heterojunction Implant with Electroâ€Mechanobiological Coupling Cues Promotes Osteogenesis. Advanced Functional Materials, 2021, 31, 2106249.	14.9	26
33	Therapeutic Potential of Circular RNAs in Osteosarcoma. Frontiers in Oncology, 2020, 10, 370.	2.8	24
34	IFN-γ/SrBG composite scaffolds promote osteogenesis by sequential regulation of macrophages from M1 to M2. Journal of Materials Chemistry B, 2021, 9, 1867-1876.	5.8	23
35	1,25-dihydroxyvitamin D <sub>3</sub> Activates MMP13 Gene Expression in Chondrocytes through p38 MARK Pathway. International Journal of Biological Sciences, 2013, 9, 649-655.	6.4	20
36	Building Osteogenic Microenvironments With Strontium-Substituted Calcium Phosphate Ceramics. Frontiers in Bioengineering and Biotechnology, 2020, 8, 591467.	4.1	20

#	Article	IF	CITATIONS
37	Biocorrosion properties of Ti–3Cu alloy in F ion-containing solution and acidic solution and biocompatibility. Rare Metals, 2019, 38, 503-511.	7.1	16
38	Regulation of Ce (â¢) / Ce (â£) ratio of cerium oxide for antibacterial application. IScience, 2021, 24, 102226.	4.1	16
39	Charge-reversal nanocomolexes-based CRISPR/Cas9 delivery system for loss-of-function oncogene editing in hepatocellular carcinoma. Journal of Controlled Release, 2021, 333, 362-373.	9.9	16
40	A Multifunctional Metallohydrogel with Injectability, Selfâ€Healing, and Multistimulusâ€Responsiveness for Bioadhesives. Macromolecular Materials and Engineering, 2018, 303, 1800305.	3.6	15
41	Improvement in antibacterial ability and cell cytotoxicity of Ti–Cu alloy by anodic oxidation. Rare Metals, 2022, 41, 594-609.	7.1	15
42	Polydopamine-Assisted Immobilization of Copper Ions onto Hemodialysis Membranes for Antimicrobial. ACS Applied Bio Materials, 2018, 1, 1236-1243.	4.6	14
43	Promoting osteogenic differentiation of BMSCs via mineralization of polylactide/gelatin composite fibers in cell culture medium. Materials Science and Engineering C, 2019, 100, 862-873.	7.3	14
44	Novel CoCrWNi alloys with Cu addition: Microstructure, mechanical properties, corrosion properties and biocompatibility. Journal of Alloys and Compounds, 2020, 824, 153924.	5.5	14
45	Antimicrobial Peptide Functionalized Conductive Nanowire Array Electrode as a Promising Candidate for Bacterial Environment Application. Advanced Functional Materials, 2019, 29, 1806353.	14.9	13
46	Local delivery of naringin in beta-cyclodextrin modified mesoporous bioactive glass promotes bone regeneration: from anti-inflammatory to synergistic osteogenesis and osteoclastogenesis. Biomaterials Science, 2022, 10, 1697-1712.	5.4	13
47	Functional Nanocomplexes with Vascular Endothelial Growth Factor A/C Isoforms Improve Collateral Circulation and Cardiac Function. Small, 2020, 16, 1905925.	10.0	12
48	Rapid and highly effective bacteria-killing by polydopamine/IR780@MnO2–Ti using near-infrared light. Progress in Natural Science: Materials International, 2020, 30, 677-685.	4.4	12
49	Antibacterial, conductive, and osteocompatible polyorganophosphazene microscaffolds for the repair of infectious calvarial defect. Journal of Biomedical Materials Research - Part A, 2021, 109, 2580-2596.	4.0	12
50	A single-cell transcriptome of mesenchymal stromal cells to fabricate bioactive hydroxyapatite materials for bone regeneration. Bioactive Materials, 2022, 9, 281-298.	15.6	12
51	Hsp90 inhibitor 17‑AAG inhibits stem cell‑like properties and chemoresistance in osteosarcoma cells via the Hedgehog signaling pathway. Oncology Reports, 2020, 44, 313-324.	2.6	12
52	Minocycline hydrochloride loaded graphene oxide enables enhanced osteogenic activity in the presence of Gram-positive bacteria, <i>Staphylococcus aureus</i> . Journal of Materials Chemistry B, 2019, 7, 3590-3598.	5.8	10
53	Effect of fluorination/oxidation level of nano-structured titanium on the behaviors of bacteria and osteoblasts. Applied Surface Science, 2020, 502, 144077.	6.1	10
54	Immunomodulation and osseointegration activities of Na2TiO3 nanorods-arrayed coatings doped with different Sr content. Bioactive Materials, 2022, 10, 323-334.	15.6	10

#	Article	IF	CITATIONS
55	Eco-friendly bacteria-killing by nanorods through mechano-puncture with top selectivity. Bioactive Materials, 2022, 15, 173-184.	15.6	10
56	Programmed NP Cell Death Induced by Mitochondrial ROS in a One-Strike Loading Disc Degeneration Organ Culture Model. Oxidative Medicine and Cellular Longevity, 2021, 2021, 1-17.	4.0	8
57	Osteoconductive and osteoinductive biodegradable microspheres serving as injectable micro-scaffolds for bone regeneration. Journal of Biomaterials Science, Polymer Edition, 2021, 32, 229-247.	3.5	7
58	Noggin, an inhibitor of bone morphogeneticÂprotein signaling, antagonizes TGF-β1 in a mouse model of osteoarthritis. Biochemical and Biophysical Research Communications, 2021, 570, 199-205.	2.1	7
59	Analysis of Immune Gene Expression Subtypes Reveals Osteosarcoma Immune Heterogeneity. Journal of Oncology, 2021, 2021, 1-9.	1.3	5
60	A comparison between two laminectomy procedures in mouse spinal cord injury on Allen's animal model. Journal of Neuroscience Methods, 2022, 368, 109461.	2.5	5
61	Time-sequential changes of differentially expressed miRNAs during the process of anterior lumbar interbody fusion using equine bone protein extract, rhBMP-2 and autograft. Frontiers of Materials Science, 2014, 8, 72-86.	2.2	2
62	Bioinks: 3D Printing of Mechanically Stable Calciumâ€Free Alginateâ€Based Scaffolds with Tunable Surface Charge to Enable Cell Adhesion and Facile Biofunctionalization (Adv. Funct. Mater. 9/2019). Advanced Functional Materials, 2019, 29, 1970053.	14.9	2
63	Correlation between motor behavior and ageâ€related intervertebral disc degeneration in cynomolgus monkeys. JOR Spine, 2022, 5, e1183.	3.2	2
64	Preparation of polycation with hydroxyls for enhanced delivery of miRNA in osteosarcoma therapy. Biomaterials Science, 2022, 10, 2844-2856.	5.4	1
65	A new method for preparing single-cell nuclear suspension of frozen spinal cord tissue. Journal of Neuroscience Methods, 2022, 370, 109490.	2.5	Ο